

## Numerical Evidence for bcc Ordering at the Surface of a Critical fcc Nucleus

Pieter Rein ten Wolde,<sup>1</sup> Maria J. Ruiz-Montero,<sup>2</sup> and Daan Frenkel<sup>1</sup>

<sup>1</sup>*FOM Institute for Atomic and Molecular Physics, Kruislaan 407, 1098 SJ Amsterdam, The Netherlands*

<sup>2</sup>*Física Teórica, Facultad de Física, Apdo. de Correos 1065, 41080 Sevilla, Spain*

(Received 2 June 1995)

We report a computer-simulation study of the crystal nucleation barrier and the structure of crystal nuclei in a Lennard-Jones system at moderate supercooling. The stable structure of the Lennard-Jones solid is known to be face-centered cubic. We find that the precritical nuclei are predominantly body-centered cubic ordered. But, as the nucleus grows to its critical size, the core becomes fcc ordered. Surprisingly, however, the interface of the critical nucleus retains a high degree of bcc-like ordering.

PACS numbers: 61.50.Cj, 02.70.Lq, 07.05.Tp

In 1897 Ostwald [1] formulated his “step” rule, stating that the crystal phase that is nucleated from the melt need not be the one that is thermodynamically most stable, but the one that is closest in free energy to the fluid phase. Stranksi and Totomanow [2] reexamined this rule and argued that the phase that will form is the one that has the lowest free-energy barrier of formation, rather than the phase that is globally stable under the conditions prevailing. More recently, Alexander and McTague [3] have argued, on the basis of Landau theory, that at least for small supercooling, nucleation of the body-centered-cubic (bcc) phase should uniquely be favored in all simple fluids exhibiting a weak first order phase transition. Also a theoretical study by Klein and Leyvraz [4] suggests that a metastable bcc phase can easily be formed from the undercooled liquid. Experimentally, nucleation of a metastable bcc phase has been observed in rapidly cooled metal melts [5].

However, when attempts were made to investigate the formation of metastable bcc nuclei on a microscopic scale, using computer simulation [6–12], the picture that emerged gave little support for the Alexander-McTague scenario. For the Lennard-Jones system, which is known to have a stable face-centered-cubic (fcc) structure up to the melting curve, the formation of a metastable bcc phase was observed in only one of the simulation studies reported [6], while all other studies [7–12] found evidence for the formation of fcc nuclei. Of particular interest is the simulation of Swope and Andersen [12] on a system comprising one million Lennard-Jones particles. This study showed that, although both fcc and bcc nuclei are formed in the early stages of the nucleation, only the fcc nuclei grow into larger crystallites. It should be noted however, that in all these simulation studies, very large degrees of supercooling (down to 50% of the melting temperature, or lower) had to be imposed to see any crystal formation on the time scale of the simulation. For such a large undercooling one should expect the free-energy barrier for nucleation into essentially all possible crystal phases to be quite small. It is therefore not obvious that crystal nucleation at large undercooling will proceed in the same way as close to the freezing point.

In the present study, homogeneous nucleation in a Lennard-Jones system closer to the freezing point is investigated. Rather than using a “brute-force” approach where we wait for nuclei to form spontaneously, we use the scheme developed by one of us [13] to study the free-energy barrier to crystal nucleation. The advantage of this technique is that it can be used even at small (i.e., realistic) undercooling where the straightforward molecular dynamics technique will not work, because the nucleation barrier diverges at coexistence. Moreover, the sampling technique that we employ [13,14] allows us to stabilize the critical nucleus and study its structure in detail.

In order to measure the free-energy barrier that separates the supercooled liquid from the solid, we must first define an order parameter which acts as a “reaction coordinate,” in the sense that it has a small value in the liquid state and a large value when the system has crystallized. Moreover, as we do not know *a priori* which crystal structure will form, we must use an order parameter that is sensitive only to the overall degree of crystallinity in the system but not to the differences between the possible crystal structures. van Duijneveldt and Frenkel [13] have shown that the bond orientational order parameter  $Q_6$  (see below), first introduced by Steinhardt, Nelson, and Ronchetti [15], satisfies these requirements and can be conveniently implemented in numerical simulations.

The Gibbs free energy of the system,  $G$ , is a function of this order parameter [16]:

$$G(Q_6) = \text{const} - k_B T \ln[P(Q_6)], \quad (1)$$

where  $P(Q_6)$  is the probability per unit interval to find the order parameter around a given value of  $Q_6$ . Both Monte Carlo (MC) and molecular dynamics (MD) simulations have been performed to measure  $P(Q_6)$ . In order to get a reliable estimate of  $P(Q_6)$  even near the top of the barrier, we used the umbrella sampling technique of Torrie and Valleau [14], in which the sampling of configuration space is biased in such a way that good statistics can be obtained for all values of  $Q_6$ .

All simulations were carried out at constant temperature and pressure. In the MD simulations this was done using the extended system method of Nosé and Andersen [17].

The MC program was based on the scheme used by van Duijneveldt and Frenkel [13]. In what follows we use reduced units, such that the Lennard-Jones well depth  $\epsilon$  is the unit of energy, while the Lennard-Jones diameter  $\sigma$  is the unit of length. In order to minimize artifacts due to the finite system size, we simulated a fairly large system, i.e., of 10 648 particles. Simulations were performed in the direction of both increasing and decreasing crystallinity. All results reported below are based on simulations that were free of hysteresis. It should be stressed, however, that, near the top of the barrier, very long simulations were required to equilibrate the system.

In our simulations, we studied the nucleation barrier under conditions of moderate (20%) supercooling, at two different pressures:  $P = 0.67$  ( $T = 0.6$ ) and  $P = 5.68$  ( $T = 0.92$ ). We find that initially, as  $Q_6$  is increased from the liquid, the number of small solid clusters in the liquid increases. The reason why there are, initially, several small solid clusters is that it is entropically favorable for the system to distribute a given amount of crystallinity over several clusters. However, as the top of the barrier is approached, the energetic factors dominate and several of these small solid clusters combine into a large one. This cluster corresponds to the critical nucleus. When  $Q_6$  is increased even further this critical nucleus grows. Figure 1 shows the Gibbs free energy of the system relative to the liquid phase, as a function of crystallinity ( $Q_6$ ). The value of the Gibbs free energy of the system at the top of the barrier corresponds to the nucleation barrier. To our knowledge this is the first numerical determination of such a nucleation barrier. We have compared the measured nucleation barrier

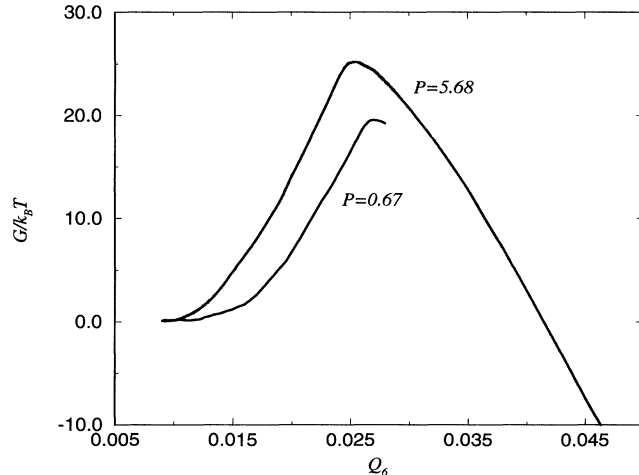


FIG. 1. The Gibbs free energy of a Lennard-Jones system as a function of crystallinity ( $Q_6$ ) at 20% undercooling for two different pressures, i.e.,  $P = 5.68$  ( $T = 0.92$ ) and  $P = 0.67$  ( $T = 0.6$ ). The Gibbs free-energy barriers are approximately  $25.1k_B T$  at  $P = 5.68$  and  $19.4k_B T$  at  $P = 0.67$ .

with the corresponding prediction of classical nucleation theory (CNT).

To make such a comparison, we need to know the solid-liquid surface free energy  $\gamma_{sl}$ . In fact,  $\gamma_{sl}$  is not known for Lennard-Jones crystals in contact with a supercooled liquid. However, Broughton and Gilmer have calculated the interfacial free energy for the Lennard-Jones fcc-liquid interface at coexistence, near the triple point (i.e., at low pressure) [18]. If we assume that we can use the Broughton-Gilmer values for  $\gamma_{sl}$  under the conditions of our simulations, CNT yields the following predictions for the nucleation barriers:  $G/k_B T = 17.4$  at  $P = 0.67$  and  $G/k_B T = 8.2$  at  $P = 5.68$ . We find from our simulations that  $G/k_B T \approx 19.4$  for the lower pressure (see Fig. 1), which is in good agreement with the theoretical prediction. The discrepancy between CNT and simulation for  $P = 5.68$  is most likely mainly due to the fact that  $\gamma_{sl}$  at this temperature and pressure is, in fact, somewhat larger ( $\approx 40\%$ ) than the Broughton-Gilmer estimate. A direct test of the CNT prediction for the size of the critical nucleus is more subtle as it depends sensitively on the criterion used to identify "solidlike" particles. Different measures of the size of the critical nucleus are compared in a forthcoming publication [19].

Next, we consider the structure of the crystal nuclei. In order to analyze the structure of a crystalline cluster, we must first determine which particles are solidlike. In previous simulation studies of homogeneous nucleation many different criteria have been used [6,8,12,20,21] to identify solidlike particles. A problem with most of these techniques is that they require an *a priori* assumption about the structure of the solid. As we wish to postpone identification of the solid structure to as late a stage as possible, we have devised a novel method that is insensitive to the type of crystalline ordering in the cluster. Details of this scheme will be discussed in Ref. [19]. Here we briefly sketch the essentials. We characterize the local structure around particle  $i$  by a set of numbers

$$\bar{q}_{lm}(i) \equiv \frac{1}{N_b(i)} \sum_{j=1}^{N_b(i)} Y_{lm}(\hat{\mathbf{r}}_{ij}), \quad (2)$$

where  $Y_{lm}(\hat{\mathbf{r}}_{ij})$  are spherical harmonics,  $\hat{\mathbf{r}}_{ij}$  is a unit vector in the direction of the bond between particle  $i$  and its neighbor  $j$ , and the sum runs over all  $N_b(i)$  neighbors. A *global* bond order parameter, such as  $Q_6$ , is obtained by computing  $\bar{Q}_{lm}$ , the average of  $\bar{q}_{lm}(i)$  over all particles, and then constructing a rotational invariant  $Q_l$  out of the  $\bar{Q}_{lm}$ :  $Q_l \equiv \left( \frac{4\pi}{2l+1} \sum_{m=-l}^l |\bar{Q}_{lm}|^2 \right)^{1/2}$ . From the  $\bar{q}_{lm}(i)$  we can, in the same way, construct an invariant  $q_l(i)$  which measures the *local* bond order around particle  $i$ . However, such a local invariant is not very useful to identify solidlike particles, because it is large not only in the solid, but also in the liquid where the *local* order remains high. The reason why, nevertheless, a *global* order parameter such as  $Q_6$  vanishes in the liquid is that

all the  $\bar{q}_{lm}(i)$  add up incoherently in the liquid. It is precisely the coherence of local bond order in a solid that we use to identify solidlike particles. To this end, we construct a normalized complex factor  $\tilde{q}_l(i)$ , with components  $\tilde{q}_{lm}(i)$  proportional to the  $\bar{q}_{lm}(i)$  defined in Eq. (2). We can now define a dot product of the vectors  $\tilde{q}_l$  of neighboring particles  $i$  and  $j$ :

$$\tilde{q}_l(i) \cdot \tilde{q}_l(j) \equiv \sum_{m=-l}^l \tilde{q}_{lm}(i) \tilde{q}_{lm}(j)^*. \quad (3)$$

Clearly,  $\tilde{q}_l(i) \cdot \tilde{q}_l(i) = 1$ . We consider two neighboring particles  $i$  and  $j$  to be “connected” if the dot product  $\tilde{q}_6(i) \cdot \tilde{q}_6(j)$  exceeds a certain threshold (in our case, 0.5). As it can happen by chance that in the liquid the vectors  $\tilde{q}_6(i)$  of neighboring particles are in phase with each other, we add an extra criterion: a particle will be identified as solidlike only if the number of “connections” with its neighboring particles exceeds a given minimum (we obtained robust results with a lower limit of seven connected neighbors).

After we have identified the solidlike clusters, we wish to characterize the local crystal structure of the clusters. To this end, we again make use of the local bond-order parameters defined above. In a perfect crystal, the local bond order is the same for all particles. However, in a crystal at finite temperature, we will find a *distribution* of local order parameter values. The nature of this distribution varies from one crystal structure to another. We have identified the local crystalline symmetry of a solid cluster as follows. We interpret the histogram of the local order parameter distribution as a vector  $\vec{v}_{\text{clus}}$  (with as many components as there are bins in the histogram). This vector, we then decompose into the *characteristic* vectors of the thermally equilibrated liquid, bcc, and fcc structures, which are denoted by  $\vec{v}_{\text{liq}}$ ,  $\vec{v}_{\text{bcc}}$ , and  $\vec{v}_{\text{fcc}}$ , respectively. In practice, we achieve this by minimizing the “distance”  $\Delta$ :

$$\Delta^2 = [\vec{v}_{\text{clus}} - (f_{\text{liq}}\vec{v}_{\text{liq}} + f_{\text{bcc}}\vec{v}_{\text{bcc}} + f_{\text{fcc}}\vec{v}_{\text{fcc}})]^2. \quad (4)$$

$f_{\text{liq}}$ ,  $f_{\text{bcc}}$ , and  $f_{\text{fcc}}$  are a measure for the type of order present in the cluster. The value of  $\Delta$  is an indication of the quality of the fit. For instance, if we were to apply our analysis to a thermally equilibrated fcc crystal, we would find  $f_{\text{fcc}} = 1$  and  $\Delta = 0$ .

We have used the above analysis to study the structure of the nuclei that form in the supercooled Lennard-Jones fluid. Here we present only the results for the system at  $P = 5.68$ . The results for  $P = 0.67$  are qualitatively similar [19]. Figure 2 shows  $f_{\text{liq}}$ ,  $f_{\text{bcc}}$ , and  $f_{\text{fcc}}$  for the largest cluster in our system as the system moves up the nucleation barrier. We note that the precritical nuclei are predominantly bcc-like with an appreciable “liquidlike” character (in the equilibrated liquid we also found small (13 particles) icosahedral clusters, but these did not grow [19]). However, near the top of the barrier there is a clear change in the nature of the solid nuclei from bcc-like to

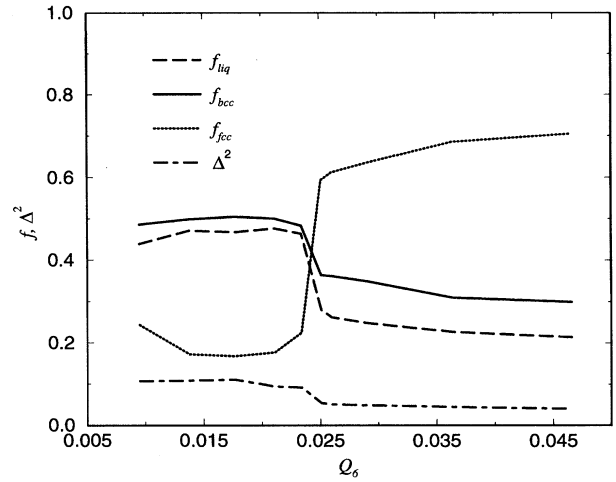


FIG. 2. Structural composition of the largest cluster, indicated by  $f_{\text{liq}}$ ,  $f_{\text{bcc}}$ ,  $f_{\text{fcc}}$ , and  $\Delta^2$ , as a function of  $Q_6$  at 20% undercooling ( $P = 5.68, T = 0.92$ ). This figure is based on averages over 50 independent atomic configurations.

fcc-like. The fact that the precritical nuclei are rather liquidlike is not very surprising as they are very small and almost all interface. What is more interesting is that these nuclei are clearly more bcc ordered than fcc ordered. This suggests that, at least for small crystallites, we find the behavior predicted by the Alexander-McTague theory [3]. Yet, as the larger clusters are increasingly fcc-like, the present results are also compatible with the findings of Swope and Andersen [12], who observed that nucleation proceeded through fcc crystallites.

Still, we note that the critical and postcritical nuclei are not fully fcc ordered. They have both appreciable liquidlike and bcc-like character. In fact, it is not surprising to find some liquidlike behavior as the nuclei still have a relatively large crystal-liquid interface. In contrast, the bcc-like character is more intriguing. We have therefore analyzed the *local* order of the critical nucleus. This is facilitated by the fact that we find our critical (and postcritical) nuclei to be quite spherical [22] (in striking contrast to the ramified structures sometimes observed at large undercooling [20,21]). Given the spherical shape of the critical and postcritical nuclei, it is meaningful to calculate  $f_{\text{liq}}$ ,  $f_{\text{bcc}}$ , and  $f_{\text{fcc}}$  in a spherical shell of radius  $r$  around the center of mass of the cluster. Figure 3 shows the radial profile of the local order of the critical nucleus. As expected, we find that the core of the nucleus is predominantly fcc-like and that  $f_{\text{liq}}$  and  $f_{\text{fcc}}$  smoothly go to one and zero, respectively, in the liquid. In fact, we find that the crystal-liquid interface is rather broad, approximately  $4\sigma$ , which is in agreement with nonclassical theories of homogeneous nucleation [23,24]. However, what is very surprising is that  $f_{\text{bcc}}$ , before decaying to zero in the liquid, increases at the interface and becomes even larger than

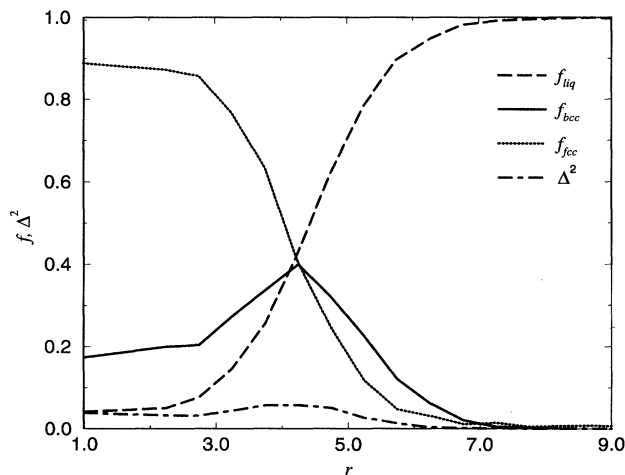


FIG. 3. Structure of the critical nucleus, indicated by  $f_{liq}$ ,  $f_{bcc}$ ,  $f_{fcc}$ , and  $\Delta^2$ , as a function of  $r$ , the distance to its center of mass, at 20% undercooling ( $P = 5.68, T = 0.92$ ). This figure is based on averages over 50 independent atomic configurations.

$f_{fcc}$ . The surface enhancement of the bcc signature is absent when we bring a fcc crystallite in contact with a liquid and do not allow the surface structure to relax. Hence, the present simulations suggest that the fcc-like core of the equilibrated nuclei is “wetted” by a shell which has more bcc character. This also explains the overall bcc character of the precritical nuclei: the structure of these small clusters is almost completely surface dominated.

In summary, our simulations indicate that homogeneous crystal nucleation in a Lennard-Jones system close to coexistence proceeds via nuclei that are initially predominantly bcc ordered. When these nuclei grow, their cores become more fcc ordered. However, in the interface a high degree of bcc ordering is retained, even in the limit of large crystals. This finding may explain why earlier simulations on small systems [6] found evidence for bcc-like crystal nuclei, while simulations on larger systems all found that crystallization proceeded through fcc nuclei [8–12].

Experimental observation of the surface structure of critical nuclei seems difficult for atomic or simple molecular liquids. However, in the case of crystallization in colloidal liquids, it should in principle be possible to image pre- and postcritical crystal nuclei, using confocal scanning laser microscopy.

This work was supported in part by “Scheikundig Onderzoek Nederland” (SON) with financial aid from NWO (“Nederlandse Organisatie voor Wetenschappelijk Onderzoek”). The work of the FOM Institute is part of the research program of “Stichting Fundamenteel

Onderzoek der Materie” (FOM) and is supported by NWO. M.J. Ruiz-Montero acknowledges partial support from EU-HCM Grant No. ERBCHWICT941060 and Grant NO. PB92-0683 from Dirección General de Investigación Científica y Técnica (Spain). We thank Joost Frenken for a critical reading of the manuscript.

- 
- [1] W. Ostwald, *Z. Phys. Chem.* **22**, 289 (1897).
  - [2] I.N. Stranski and D. Totomanow, *Z. Phys. Chem.* **163**, 399 (1933).
  - [3] S. Alexander and J.P. McTague, *Phys. Rev. Lett.* **41**, 702 (1978).
  - [4] W. Klein and F. Leyvraz, *Phys. Rev. Lett.* **57**, 2845 (1986).
  - [5] R.E. Cech, *J. Met.* **8**, 585 (1956).
  - [6] M.J. Mandell, J.P. McTague, and A. Rahman, *J. Chem. Phys.* **66**, 3070 (1977).
  - [7] M.J. Mandell, J.P. McTague, and A. Rahman, *J. Chem. Phys.* **64**, 3699 (1976).
  - [8] C.S. Hsu and A. Rahman, *J. Chem. Phys.* **71**, 4974 (1979).
  - [9] R.D. Mountain and A.C. Brown, *J. Chem. Phys.* **80**, 2730 (1984).
  - [10] S. Nosé and F. Yonezawa, *J. Chem. Phys.* **84**, 1803 (1986).
  - [11] J. Yang, H. Gould, and W. Klein, *Phys. Rev. Lett.* **60**, 2665 (1988).
  - [12] W.C. Swope and H.C. Andersen, *Phys. Rev. B* **41**, 7042 (1990).
  - [13] J.S. van Duijneveldt and D. Frenkel, *J. Chem. Phys.* **96**, 4655 (1992).
  - [14] G.M. Torrie and J.P. Valleau, *Chem. Phys. Lett.* **28**, 578 (1974).
  - [15] P.J. Steinhardt, D.R. Nelson, and M. Ronchetti, *Phys. Rev. B* **28**, 784 (1983).
  - [16] L.D. Landau and E.M. Lifshitz, *Statistical Physics* (Pergamon, London, 1980), 3rd ed.
  - [17] S. Nosé, in *Computer Simulations in Materials Science*, edited by M. Meyer and V. Pontikis (Kluwer, Dordrecht, 1991), pp. 21–41.
  - [18] J.Q. Broughton and G.H. Gilmer, *J. Chem. Phys.* **84**, 5759 (1986).
  - [19] P.R. ten Wolde, M.J. Ruiz-Montero, and D. Frenkel (to be published).
  - [20] J.D. Honeycutt and H.C. Andersen, *J. Phys. Chem.* **90**, 1585 (1986).
  - [21] J. Yang, H. Gould, W. Klein, and R.D. Mountain, *J. Chem. Phys.* **93**, 711 (1990).
  - [22] Unlike Báez and Clancy [*J. Chem. Phys.* **102**, 8138 (1995)], we find no evidence for octahedral nuclei (see Ref. [19]).
  - [23] P. Harrowell and D.W. Oxtoby, *J. Chem. Phys.* **80**, 1639 (1984).
  - [24] C.K. Bagdassarian and D.W. Oxtoby, *J. Chem. Phys.* **100**, 2139 (1994).